ACTA ACUSTICA UNITED WITH ACUSTICA
Vol. 90 (2004) 410 – 418

# Analysis of the Burgers Equation Applied to Parametric Transmission: Influence of the Phase of the Primary Waves and Sub-Harmonics Generation

Jacques Marchal, Pierre Cervenka
Laboratoire de Mécanique Physique associé au CNRS (UMR 7068), Université Pierre et Marie Curie, 2 place de la gare de ceinture, 78210 Saint-Cyr-l'Ecole, France

**Summary**
The solution of the Burgers equation is investigated to analyze the parametric conversion of plane progressive waves in thermo-viscous media. The particular cases of integral and half-integral parametric frequency ratios are studied: the influence of the initial phasing of the primary waves on the efficiency of the parametric conversion is pointed out; the mechanism of the sub-harmonics generation is also described. In the general case, it is shown that these effects are significant when the parametric ratio is small.

**PACS no. 43.25.Cb, 43.25.Lj**

## 1. Introduction

The original idea of parametric transmission has been introduced by Westervelt [1] in the 60', and has been since much studied (e.g. [2]). The principle consists of taking advantage of the nonlinear interaction of two harmonic – so-called primary – beams, in order to create a radiation at the difference frequency. The 1-D model is convenient to explicit the mechanism of the parametric conversion, as well as the transfers of energy towards linear combinations of harmonics.

In a thermo-viscous medium, the nonlinear propagation of plane waves is described by the Burgers equation [3] whose general solution is known. Many studies have been performed with various initial conditions, e.g. single-frequency source [4], bi-harmonic source (i.e. $\omega$ and $2\omega$) [5], parametric transmission [6], and multi-frequency sources [7]. In this paper, one uses the solution of the Burgers equation that applies in the parametric case to point out and to explain several phenomena that can have a critical impact in the optimization of actual parametric transmitters. One focuses particularly on the influence of the initial phasing between the primary waves. Rudenko [5] and Hedberg [8] spotted this influence with bi-harmonic emission. In the case of parametric transmission, it is shown in this paper that the efficiency of the conversion depends significantly on the phasing when the primary-to-secondary frequencies ratio (hereafter called parametric ratio) is small. The mechanism that leads to the generation of sub-harmonics whose frequencies are smaller than the difference frequency between the primary waves is also analyzed.

The solution of the Burgers equation that applies in parametric transmission is first recalled in section 2. The parametric ratio is then formulated as a rational number to show how subharmonics appear. The case of half-integral parametric ratio is thoroughly detailed in section 3. The interest of this particular figure is that the spectrum of the propagating signal contains only multiples of the difference frequency. The parametric efficiency is analyzed in function of the parametric ratio, of the source level, and of the initial phase between the primary waves. The evolution of the shape of the propagating wave is discussed. The asymptotic behavior of the harmonics is described. Section 4 deals with the simplest case for which one single sub-harmonic is created, namely when the parametric ratio is an integer. The effect of this sub-harmonic wave on the evolution of the parametric wave is discussed. Results obtained in sections 3 and 4 provide the basis for an interpretation in section 5 of how the parametric conversion can vary in the general case, i.e. with non-integral and non half-integral parametric ratios.

## 2. Burgers equation and parametric transmission

In a thermo-viscous fluid, the 1-D propagation along the $z$-axis is modeled by the classical Burgers equation. Let us denote $U$ the dimensionless velocity that is related to the velocity $V$ through the Mach number $M$ by $V = Mc_0U$

Received 25 September 2003,
accepted 15 November 2003.

($c_0$ is the sound speed in the medium). The Burgers equation reads

$$\frac{\partial U}{\partial z} = \frac{b}{2\rho_0 c_0^3}\frac{\partial^2 U}{\partial \tau^2} + \frac{\beta M}{c_0} U \frac{\partial U}{\partial \tau}, \tag{1}$$

where $\tau = t - z/c_0$ is the retarded time ($t$ is the actual time); $\beta$ is the coefficient of nonlinearity of the medium ($\beta \approx 3.5$ in water); $b$ is a constant proportional to the coefficients of viscosity and heat conduction. The linear attenuation coefficient for a wave at the angular frequency $\omega$ is proportional to $b$, and quadratic with $\omega$:

$$\alpha_\omega = \frac{b\omega^2}{2\rho_0 c_0^3}, \tag{2}$$

($\rho_0$ is the density of the fluid).

In the parametric transmission problem, the initial signal at $z = 0$ consists of two harmonic waves at frequencies $\omega_{p_1}$ and $\omega_{p_2}$ ($> \omega_{p_1}$):

$$V(z=0,t) = V_{p_1}^{(0)} \sin(\omega_{p_1} t) + V_{p_2}^{(0)} \sin(\omega_{p_2} t + \varphi). \tag{3}$$

$V_{p_1}^{(0)}$ and $V_{p_2}^{(0)}$ are the initial amplitude of the velocities, and $\varphi$ is an initial phase. The mean primary frequency is denoted

$$\Omega = (\omega_{p_1} + \omega_{p_2})/2. \tag{4}$$

The interest of the parametric transmission is the creation of the wave at the difference frequency

$$\omega_- = \omega_{p_2} - \omega_{p_1}. \tag{5}$$

The parametric ratio $\mu$ is defined by

$$\mu = \Omega/\omega_-. \tag{6}$$

Note that the condition of practical interest $\omega_{p_1} > \omega_-$ implies $\mu > 1.5$ (so that there is also $\omega_{p_2} < 2\omega_{p_1}$).

The mean Mach number associated with the initial condition given in equation (3) is

$$M = \frac{V_{p_1}^{(0)} + V_{p_2}^{(0)}}{2c_0}. \tag{7}$$

The shock distance $l_s$ and the attenuation length $l_a$ are defined respectively by

$$l_s = \frac{c_0}{\beta M \Omega} \quad \text{and} \quad l_a = \alpha_\Omega^{-1}. \tag{8}$$

The relative influence of the nonlinearity versus the attenuation is characterized by the ratio of these distances, namely the Goldberg number

$$\Gamma = \frac{l_a}{l_s} = \frac{2\beta M \rho_0 c_0^2}{b\Omega}. \tag{9}$$

Solutions of the Burgers equation have been developed by several authors, e.g. Blackstock [4] and Novikov [9]. The trick consists of introducing the Hopf-Cole transform [10, 11]:

$$\begin{aligned} U &= \frac{2}{\Omega\Gamma}\frac{\partial \ln(\zeta)}{\partial \tau} \Leftrightarrow \\ \zeta &= \exp\left(\frac{\Omega\Gamma}{2}\int U \,\mathrm{d}\tau + \text{const.}\right), \end{aligned} \tag{10}$$

so that equation (1) turns into the diffusion equation

$$\zeta_z - \frac{b}{2\rho_0 c_0^3}\zeta_{\tau\tau} = 0. \tag{11}$$

The initial condition given in equation (3) turns into

$$\begin{aligned} \zeta(z=0,\tau) = \zeta_0 \exp\Big( &- \frac{\Gamma_{p_1}}{2}\cos(\omega_{p_1}\tau) \\ &- \frac{\Gamma_{p_2}}{2}\cos(\omega_{p_2}\tau + \varphi)\Big), \end{aligned} \tag{12}$$

where

$$\Gamma_{p_1} = U_{p_1}^{(0)}\frac{\Omega}{\omega_{p_1}}\Gamma \quad \text{and} \quad \Gamma_{p_2} = U_{p_2}^{(0)}\frac{\Omega}{\omega_{p_2}}\Gamma. \tag{13}$$

By using the relation

$$\mathrm{e}^{-a\cos\theta} = \sum_{n=-\infty}^{+\infty} (-1)^n I_n(a) \exp\left(\mathrm{j}n\theta\right), \tag{14}$$

where $I_n$ are the modified Bessel functions, equation (12) is written

$$\begin{aligned} \zeta(z=0,\tau) = \zeta_0 \sum_{k=-\infty}^{+\infty}\sum_{l=-\infty}^{+\infty} &(-1)^{k+l} I_k\left(\frac{\Gamma_{p_1}}{2}\right) \\ &\cdot I_l\left(\frac{\Gamma_{p_2}}{2}\right)\mathrm{e}^{\mathrm{j}(k\omega_{p_1}+l\omega_{p_2})\tau + \mathrm{j}l\varphi}. \end{aligned} \tag{15}$$

The integration of equation (11) yields finally the solution that can be found in [6, equation 3.23]:

$$\begin{aligned} \zeta(z,\tau) = \zeta_0 \sum_{k=-\infty}^{+\infty}\sum_{l=-\infty}^{+\infty} &(-1)^{k+l} I_k\left(\frac{\Gamma_{p_1}}{2}\right) \\ &\cdot I_l\left(\frac{\Gamma_{p_2}}{2}\right)\mathrm{e}^{-\alpha_{k\omega_{p_1}+l\omega_{p_2}} z}\mathrm{e}^{\mathrm{j}(k\omega_{p_1}+l\omega_{p_2})\tau + \mathrm{j}l\varphi}. \end{aligned} \tag{16}$$

Note that this result could have been obtained by solving first equation (1) with the initial conditions equation (12) but without introducing any phase ($\varphi = 0$). Then, the general solution given in equation (16) for any phase $\varphi$ can be derived straightforwardly by using the phase theorem [12].

The solution $U$ is finally obtained by applying the inverse transform (10) to equation (16):

$$U(z,\tau) = \frac{2}{\Gamma\Omega}\frac{N}{D}, \tag{17}$$

with

$$\begin{aligned} D = \sum_{k=-\infty}^{+\infty}\sum_{l=-\infty}^{+\infty} &(-1)^{k+l} I_k\left(\frac{\Gamma_{p_1}}{2}\right) I_l\left(\frac{\Gamma_{p_2}}{2}\right) \\ &\cdot \mathrm{e}^{-\alpha_{k\omega_{p_1}+l\omega_{p_2}} z}\cos\left((k\omega_{p_1} + l\omega_{p_2})\tau + l\varphi\right), \end{aligned} \tag{18}$$

and

$$N = \frac{\mathrm{d}D}{\mathrm{d}\tau}. \tag{19}$$

Equation (18) involves an infinite set of pulsations that is difficult to sort. However, it is always possible to approximate the ratio of the primary frequencies with a rational number, $\omega_{p_1}/\omega_{p_2} = p/q$, where $p$ and $q$ are reciprocal prime numbers. Doing so, all frequencies are multiple of a reference pulsation denoted $\omega$, and the primary frequencies are equal to

$$\omega_{p_1} = p\omega \quad \text{and} \quad \omega_{p_2} = q\omega. \tag{20}$$

Let us recall that in the specific case of parametric transmission, there is $p < q < 2p$. For now, the notation $\omega_n = n\omega$ is used, so that $\omega_{p_1} = \omega_p$ and $\omega_{p_2} = \omega_q$. Note that the initial signal equation (3) is periodic, with the period $2\pi/\omega$.

Let us introduce the notation

$$\varepsilon(z) = \mathrm{e}^{-\alpha_\omega z}. \tag{21}$$

Keeping in mind that the attenuation coefficient is quadratic with the frequency (equation 2, equation 18) reads

$$D = \sum_{k=-\infty}^{+\infty} \sum_{l=-\infty}^{+\infty} (-1)^{k+l} I_k\left(\frac{\Gamma_{p_1}}{2}\right) \cdot I_l\left(\frac{\Gamma_{p_2}}{2}\right) \varepsilon^{(lq+kp)^2} \cos\big((lq+kp)\omega\tau + l\varphi\big). \tag{22}$$

$N$ and $D$ can be also written in terms of the following harmonic series:

$$D = \sum_{k=0}^{+\infty} D_k \quad \text{with } D_k = f_k \varepsilon^{k^2} \cos(k\omega\tau + g_k), \tag{23}$$

$$N = \sum_{k=0}^{+\infty} N_k \quad \text{with } N_k = -k\omega f_k \varepsilon^{k^2} \sin(k\omega\tau + g_k). \tag{24}$$

There is in particular

$$\begin{aligned} D_0 &= \sum_{k=-\infty}^{+\infty} (-1)^{k(q-p)} I_{kq}\left(\frac{\Gamma_{p_1}}{2}\right) \cdot I_{kp}\left(\frac{\Gamma_{p_2}}{2}\right) \cos\big(kp\varphi\big), \\ N_0 &= 0, \end{aligned} \tag{25}$$

$$\begin{aligned} D_{q-p} &= 2\sum_{k=-\infty}^{+\infty} (-1)^{k(q-p)} I_{kq+1}\left(\frac{\Gamma_{p_1}}{2}\right) \cdot I_{kp+1}\left(\frac{\Gamma_{p_2}}{2}\right) \varepsilon^{(q-p)^2} \cdot \cos\big((q-p)\omega\tau + (kp+1)\varphi\big), \\ N_{q-p} &= \frac{\mathrm{d}D_{q-p}}{\mathrm{d}\tau}. \end{aligned} \tag{26}$$

The spectrum of the signal $U(z,\tau)$ contains all the harmonics at multiple frequencies of the reference $\omega$. Hence, the nonlinear process can build sub-harmonics whose frequencies are lower than the parametric frequency $\omega_- = \omega_{q-p}$ whenever $q - p > 1$. For now, $U_k$ denotes the component at frequency $k\omega$:

$$U(z,\tau) = \sum_{k=1}^{+\infty} U_k(z,\tau). \tag{27}$$

In the remaining part of the paper, one considers only equal amplitudes of the primary waves at the origin, i.e. $V_{p_1}^{(0)} = V_{p_2}^{(0)} = V^{(0)}$. The dimensionless waves are thus normalized, i.e. $U_{p_1}(z=0,\tau) = \sin(\omega_{p_1}\tau)$ and $U_{p_2}(z=0,\tau) = \sin(\omega_{p_2}\tau + \varphi)$. The associated Goldberg numbers equation (13) reduce to

$$\Gamma_{p_1} = \left(1 - \frac{1}{2\mu}\right)^{-1}\Gamma \quad \text{and} \quad \Gamma_{p_2} = \left(1 + \frac{1}{2\mu}\right)^{-1}\Gamma. \tag{28}$$

The above values are very close to $\Gamma$ whenever the parametric ratio $\mu$ is larger than a few units.

## 3. Half-integral parametric ratio

Whenever $\mu = p + 1/2$, there is necessarily $q = p + 1$ because $p$ and $q$ are reciprocal prime numbers. Consequently, the wave that is created at the smallest frequency is the parametric wave itself ($\omega_- = \omega$). No sub-harmonic appears. Rudenko [5] studied the bi-harmonic source that corresponds to the very special case $\mu = 1.5$ ($p = 1$, $q = 2$). It can be considered as a degenerated case of parametric transmission because $\omega_- = \omega_{p_1}$. This paper deals only with $p > 1$.

### 3.1. Parametric efficiency

Whenever the distance $z$ is large enough, an ordering of the magnitudes in the spectral decomposition of $N$ and $D$ (equations 23 and 24) takes place. The asymptotic behavior of the wave at the parametric frequency $U_1^{(\infty)}$ is thus dictated by the ratio of the only first terms in the series $N$ and $D$, i.e. $N_{1=q-p}$ and $D_0$. Using equations (25), (26) with $q = p + 1$, one derives ($\forall p > 0$)

$$\begin{aligned} U(z,\tau) \underset{z\to\infty}{\sim} U_1^{(\infty)}(z,\tau) &= \varepsilon\eta\sin(\omega\tau + \varphi + \psi) \\ &= \frac{2}{\Gamma\Omega}\frac{N_1}{D_0}, \end{aligned} \tag{29}$$

where $\eta$ and $\psi$ are defined by

$$\eta\mathrm{e}^{\mathrm{j}\psi} = \frac{4}{\mu\Gamma}\frac{\sum_{k=-\infty}^{+\infty}(-1)^{k+1} I_{kq+1}\left(\frac{\Gamma_{p_1}}{2}\right) I_{kp+1}\left(\frac{\Gamma_{p_2}}{2}\right)\mathrm{e}^{\mathrm{j}kp\varphi}}{\sum_{k=-\infty}^{+\infty}(-1)^{k} I_{kq}\left(\frac{\Gamma_{p_1}}{2}\right) I_{kp}\left(\frac{\Gamma_{p_2}}{2}\right)\cos(kp\varphi)}, \quad (q = p+1, \mu = p + 1/2). \tag{30}$$

Recalling that the dimensionless wave at the origin is $U(z=0,\tau) = \sin(\omega_{p_1}\tau) + \sin(\omega_{p_t}\tau + \varphi)$, $\eta$ appears to be the efficiency of the parametric conversion. Equation (30) shows that $R = \eta\mathrm{e}^{\mathrm{j}\psi}$ is periodic with $\varphi$ modulo $2\pi/p$. In addition, there is the symmetry $R(\varphi) = R^*(-\varphi)$, which furthermore implies $R(\varphi + \pi/p) = R^*(-\varphi + \pi/p)$. It is

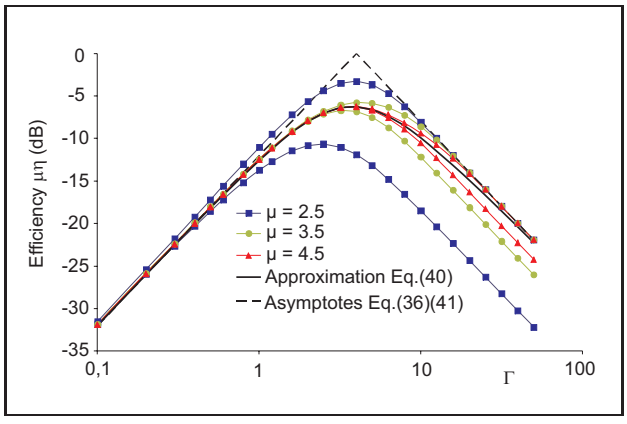


Figure 1. $\mu\eta_{\min}(\Gamma)$ and $\mu\eta_{\max}(\Gamma)$ computed with equations (32), (33), and the approximation for large $\mu$ (equation 40). Asymptotic behavior for $\Gamma \ll 1$ (equation 36) and for $\Gamma \gg \Gamma_{\max}$ (equation 41).

then sufficient to study the efficiency $\eta$ as a function of the initial phase $\varphi$ in the domain $[0, \pi/p]$. It can be shown that the extrema of $\eta(\varphi)$ are reached at the boundaries of this interval, i.e.

$$\frac{\partial \eta}{\partial \varphi}(\varphi = 0 \mathrm{mod} \pi/p) = 0. \tag{31}$$

There is

$$\eta_{\min}(\Gamma) = \eta(\varphi = 0, \Gamma) = \tag{32}$$
$$\frac{4}{\mu\Gamma} \frac{\sum_{k=-\infty}^{+\infty} (-1)^k I_{kq+1}\left(\frac{\Gamma_{p_1}}{2}\right) I_{kp+1}\left(\frac{\Gamma_{p_2}}{2}\right)}{\sum_{k=-\infty}^{+\infty} (-1)^k I_{kq}\left(\frac{\Gamma_{p_1}}{2}\right) I_{kp}\left(\frac{\Gamma_{p_2}}{2}\right)},$$
$$\eta_{\max}(\Gamma) = \eta(\varphi = \pi/p, \Gamma) = \tag{33}$$
$$\frac{4}{\mu\Gamma} \frac{\sum_{k=-\infty}^{+\infty} I_{kq+1}\left(\frac{\Gamma_{p_1}}{2}\right) I_{kp+1}\left(\frac{\Gamma_{p_2}}{2}\right)}{\sum_{k=-\infty}^{+\infty} I_{kq}\left(\frac{\Gamma_{p_1}}{2}\right) I_{kp}\left(\frac{\Gamma_{p_2}}{2}\right)}.$$

In order to examine the evolution of the parametric efficiency with the Goldberg number $\Gamma$, the function $\mu\eta(\Gamma)$ is displayed Figure 1 for several values of $p$ (i.e. half-integral parametric ratios $\mu$). Because the efficiency depends also on the initial phase $\varphi$, the lower and upper limits, $\mu\eta_{\min}(\Gamma)$ and $\mu\eta_{\max}(\Gamma)$, are presented.

In the vicinity of the origin ($\Gamma \ll 1$), the efficiency can be approximated by using in equation (30) the development of the modified Bessel functions as series

$$I_k(x) = \sum_{l=0}^{\infty} \frac{1}{l!(k+l)!} \left(\frac{x}{2}\right)^{k+2l}. \tag{34}$$

Taking into account equation (28), one obtains

$$\mu\eta = \frac{\Gamma_{p_1}\Gamma_{p_2}}{4\Gamma} = \left(1 - \frac{1}{4\mu^2}\right)^{-1} \frac{\Gamma}{4}, \quad \text{and } \psi = \pi. \tag{35}$$

Hence, the efficiency does not depend on the initial phase $\varphi$ when $\Gamma \ll 1$. Equation (35) can be furthermore simplified according to

$$\mu\eta\big|_{\Gamma \ll 1} = \Gamma/4, \tag{36}$$

because the largest error that this approximation introduces is smaller than 0.35 dB (with $\mu = 2.5$). This is indeed the asymptotic behavior that is observed close to the origin in Figure 1, where all curves are almost superimposed.

The result given by equation (35) can be also directly obtained in the weak nonlinear interaction model (e.g. [6, Chap.3 Part 2]). The wave at the difference frequency is assumed to be created by the only interaction of the primary waves. The latters are also assumed to obey the linear wave equation, i.e. there is no extra-attenuation. Using the discrete frequency notation, the primary waves read

$$\begin{aligned} U_p &= \exp\left(-\alpha_p z\right) \sin\left(p\omega\tau\right), \\ U_q &= \exp\left(-\alpha_q z\right) \sin\left(q\omega\tau + \varphi\right). \end{aligned} \tag{37}$$

The wave at the difference frequency is obtained by solving equation (1), which reads here

$$\left(\frac{\partial}{\partial z} - \frac{b}{2\rho_0 c_0^3}\frac{\partial^2}{\partial \tau^2}\right) U_1 = \frac{-\beta M \omega}{2c_0} \mathrm{e}^{-(\alpha_p+\alpha_q)z} \sin\left(\omega\tau + \varphi\right). \tag{38}$$

The solution is

$$U_1 = -\eta \mathrm{e}^{-\alpha_1 z}\left(1 - \mathrm{e}^{-(\alpha_p+\alpha_q-\alpha_1)z}\right) \sin\left(\omega\tau + \varphi\right), \tag{39}$$

where $\eta$ is the efficiency given by equation (35) that is derived from equation (30) when $\Gamma \ll 1$.

But for the vicinity of the origin, the analytical study of equation (30) is cumbersome. However, numerical simulations show the definite existence of a single maximum in the curves $\mu\eta(\Gamma)$. The efficiency grows linearly with $\Gamma$ in the vicinity of the origin. With larger source levels, nonlinear interactions increase the amount of energy transferred towards higher harmonics. This phenomenon – so called extra-attenuation – leads finally to reduce the parametric efficiency.

With small parametric ratios ($\mu = 2.5 \ldots 5.5$), and out of the weak nonlinear interaction regime, the efficiency depends significantly on the initial phase. Given the parametric ratio, $\eta_{\max}(\Gamma)/\eta_{\min}(\Gamma)$ begins to increase with $\Gamma$, and then tends towards a finite limit. In addition whatever the parametric ratio is, all functions $\mu\eta(\Gamma)$ exhibits past their maximum the same decreasing roll off in $1/\Gamma$.

The phase dependency of the efficiency tends to vanish with increasing parametric ratios. Actually, the curves $\mu\eta_{\min}(\Gamma)$ and $\mu\eta_{\max}(\Gamma)$ are indistinguishable (less than 1 dB difference) as soon as $\mu > 6.5$. Whatever the abscissa $\Gamma$ is, these curves converge towards the function that is obtained by keeping the first term in the numerator and in the

denominator of equation (30):

$$\mu\eta\Big|_{\mu\gg 1} = \frac{4}{\Gamma}\frac{I_1\left(\frac{\Gamma}{2}\right)I_1\left(\frac{\Gamma}{2}\right)}{I_0\left(\frac{\Gamma}{2}\right)I_0\left(\frac{\Gamma}{2}\right)}. \tag{40}$$

This result has been also established in [6, equation 3.24]. This function does not depend on the initial phase $\varphi$, nor on the parametric ratio $\mu$. Its maximum is equal to $-6.2$ dB, and is reached at the abscissa $\Gamma_{\max} = 3.8$. This function tends indeed towards the function $\Gamma/4$ when $\Gamma \ll \Gamma_{\max}$ (cf. equation 36). On the other hand, its asymptotic behavior for $\Gamma \gg \Gamma_{\max}$ is given by

$$\mu\eta\Big|_{\substack{\mu\gg 1\\ \Gamma\gg\Gamma_{\max}}} = 4/\Gamma. \tag{41}$$

### 3.2. Influence of the initial phase ($\mu$ = 2.5)

The dependency of the efficiency on the initial phasing of the primary waves is only significant when the parametric ratio is small. The most remarkable configuration with half integer ratios is thus obtained with $\mu = 2.5$. Figure 2 displays the corresponding mapping of $\eta(\varphi, \Gamma)$. It shows that choosing a null initial phase induces a significant discrepancy of efficiency. Actually, the observed loss occurs only within a small range of the phase domain, i.e. about [0, 10°]. Out of this domain, the efficiency remains nearly a constant ($\approx \eta_{\max}$). The magnitude of the difference $\eta_{\max}/\eta_{\min}$ is around 10 dB when $\Gamma > \Gamma_{\max}$.

The dependency of the parametric efficiency on the initial phase can be explained by observing the evolution of the signal along the $z$-axis. The source signal can be considered as an amplitude-modulated harmonic wave of pulsation $\Omega$, as it can be seen in writing equation (3) according to

$$U(z=0, \tau-\Delta\tau) = \\ 2\cos\left(1/2\omega_-\tau\right)\sin\left(\Omega\tau - (\mu-1/2)\varphi\right) \tag{42}$$

(the time shift $\Delta\tau = \varphi/\omega_-$ is only introduced here to allow a proper superimposition of the modulating envelopes). In Figure 3, the first frame displays the initial signal over the complete period of recurrence $T = 2\pi/\omega_-$, in the two extreme configurations $\varphi = 0$ and $\varphi = \pi/2$.

Let us recall that non-linearity is equivalent to local variations of the celerity $\Delta c = \beta V$. Parts of the wave where the acoustic velocity is positive propagate faster than parts where the velocity is negative. The generation of the parametric wave is thus closely linked to the gradient of amplitude induced by the envelope of the signal. More specifically, it is the asymmetry between high and low pressure zones that build the parametric wave. In both considered cases ($\varphi = 0$ and $\varphi = \pi/2$), $U(\tau - \Delta\tau)$ is anti-symmetric whereas the deformations that the signal undergoes are symmetric. Consequently, the wave created at the difference frequency is antisymmetric, e.g. null at the origin. Figure 3 shows the comparative evolution of $U(z, \tau)$, computed at several distances with $\Gamma = 5$: looking at each half part of the signal, the shape of the signal whose initial phasing equals $\pi/2$ appears to be more appropriate for

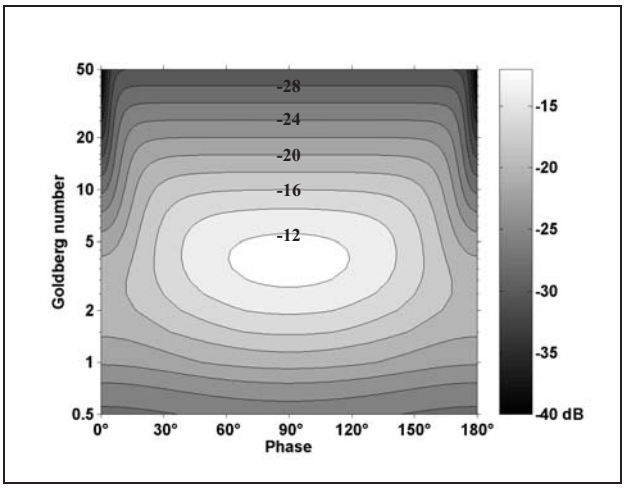


Figure 2. Mapping of efficiency $\eta(\varphi, \Gamma)$ with parametric ratio $\mu = 2.5$.

building the secondary wave. One can guess that the advantage afforded by one configuration over another one tends to disappear when the number of oscillations inside the envelope of modulation increases (i.e. larger $\mu$).

The far range magnitude of $U$ (last frame in Figure 3) is in the ratio 1 to 3 when comparing the initial phase $\varphi = 0$ versus $\varphi = \pi/2$. Because $U$ is there reduced to the harmonic $U_1$, this value is indeed consistent with the 9 dB difference of efficiency that can be observed with $\Gamma = 5$ in the curves of Figure 1 and in the mapping displayed Figure 2. However, the influence of the initial phase is already significant at closer range, in the vicinity of the primary waves. Figure 4 displays the evolution with range of the magnitudes of $U_1$ in both cases ($\varphi = 0$ and $\varphi = \pi/2$). In the presented simulation, half of the difference of efficiency is already reached at one attenuation length ($z \approx l_a = 5l_s$). The difference is almost completely settled at a range of a few attenuation lengths ($z \approx 3l_a = 15l_s$).

### 3.3. Asymptotic behavior of harmonics ($\mu = p + 1/2$)

The asymptotic behavior of each spectral component of the signal $U(z, \tau)$ can be estimated for large $z$. Equation (17) is developed in terms of powers of $\varepsilon$ defined in equation (21). Sorting the components associated to a given frequency $k\omega$, the asymptotic form $U_k^{(\infty)}$ is obtained by keeping the term that corresponds to the lowest power of $\varepsilon$. It can be checked that the solutions are derived from the product of $N_1$ by the $\varepsilon^{k-1}$ term of the development of $(D_0 + D_1)^{-1}$. Using the notations introduced in equation (29), one finds after some cumbersome calculations:

$$U_k^{(\infty)} = \varepsilon^k \left(\frac{\mu\Gamma}{4}\right)^{k-1} \eta^k \sin\left(k(\omega\tau + \varphi + \psi)\right). \tag{43}$$

This equation shows that the harmonic $k\omega$ follows the asymptotic law $\varepsilon^k = \exp(-k\alpha_\omega z)$, which is different than the thermo-viscous attenuation $\exp(-k^2\alpha_\omega z) = \varepsilon^{k^2}$. This result is analog to the asymptotic behavior given by

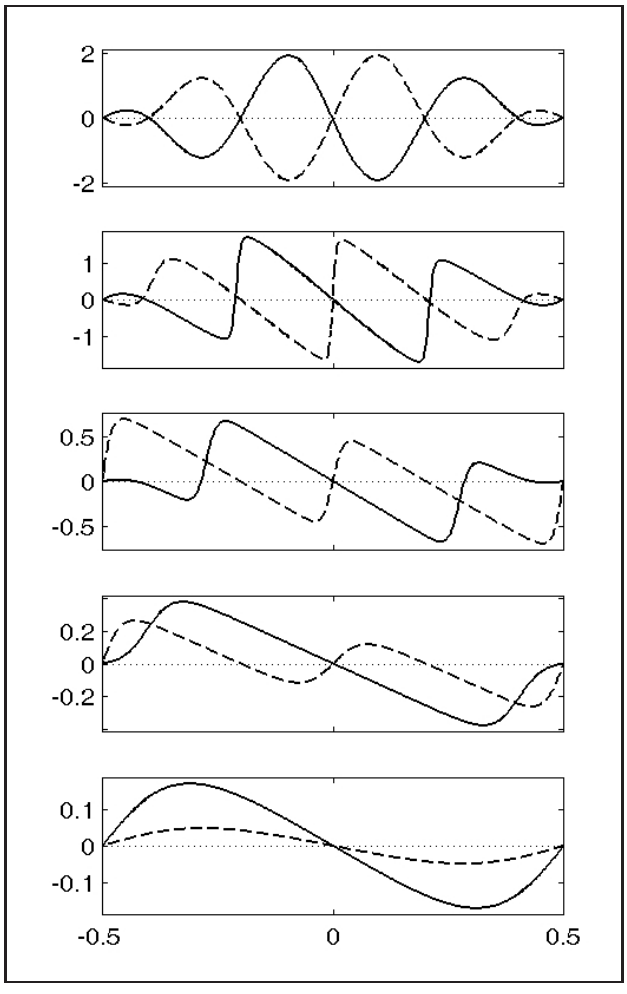


Figure 3. $\varepsilon^{-1}U(z,\tau)$ with $\mu = 2.5$ and $\Gamma = 5$ (normalized abscissa $\tau/T$). Solid line: $\varphi = 0$; Dashed line: $\varphi = \pi/2$. From top to bottom: $z/l_s$ = 0, 1, 5, 15, $\infty$.

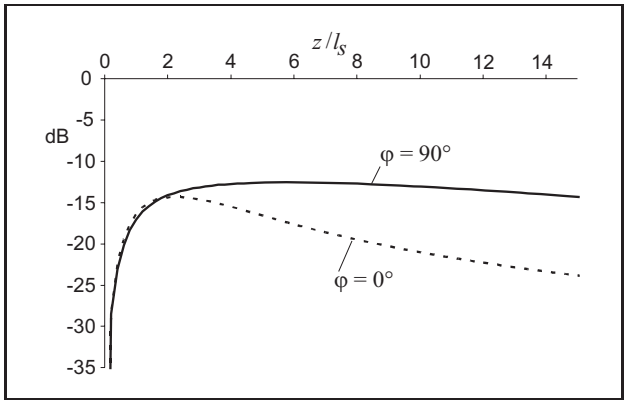


Figure 4. Evolution of the amplitude of the first harmonic $U_1$ ($\mu = 2.5, \Gamma = 5$). Comparison between initial phases $\varphi = 0$ and $\varphi = 90°$.

the Fay solution [13] that applies with a single harmonic source. The fundamental harmonic $\omega$ obeys the classical absorption in a lossy fluid. The upper harmonics $k\omega$ are fed by nonlinear interactions, most of the contributions coming from interactions between harmonics of lower ranks.

Taking into account the ordering that takes place at far range, the level of the parametric wave $\omega_- = \omega$ overcomes all the other harmonics when the parametric ratio is a half-integer.

## 4. Integral parametric ratio

Given an integral parametric ratio ($\mu = m > 1$, $m$ integer), there is necessarily $p = 2m - 1$ and $q = 2m + 1$ because $p$ and $q$ are reciprocal prime numbers. The smallest frequency that is generated is now half the parametric frequency ($\omega = \omega_-/2$). The asymptotical behavior of the components at frequency $k\omega$ can be analyzed as before by considering the development of the solution equation (17) in powers of $\varepsilon = \exp(-\alpha_\omega z)$. For large $z$, it gives the same ordering in the spectral components:

$$U_k^{(\infty)} \propto \varepsilon^k. \tag{44}$$

Consequently, the parametric wave $U_2$, i.e. at frequency $2\omega$, does not have the largest amplitude at far range. It is the sub-harmonic $U_1$ at frequency $\omega$ that overcomes all the other harmonics. When the parametric ratio is a half-integer, it has been seen in the previous section that the parametric wave follows the decreasing law $\exp(-\alpha_{\omega_-} z)$. When the ratio $\mu$ is an integer, the existence of the sub-harmonic at frequency $\omega_-/2$ modifies this behavior, which turns into $\exp(-\alpha_{\omega_-} z/2)$. In order to investigate more thoroughly the evolution of the parametric wave, components at frequencies $\omega$ and $\omega_- = 2\omega$ must be studied together. Using the notation introduced in equations (23), (24), the solution equation (17) is developed up to the 4th order that corresponds to the linear attenuation of the parametric wave:

$$U(z,\tau) = \frac{2}{\Gamma\Omega}\frac{N_1 + N_2}{D_0 + D_1} + O(\varepsilon^4), \tag{45}$$

where $D_0$ and $N_{2=q-p}$ are given by equations (25), (26) computed here with $p = 2m - 1$ and $q = 2m + 1$. $D_1$ and $N_1$ are given by:

$$\begin{aligned} D_1 &= -2\varepsilon \sum_{k=-\infty}^{+\infty} I_{k(2m+1)+m}\left(\frac{\Gamma_{p_1}}{2}\right) \\ &\qquad \cdot I_{k(2m-1)+m-1}\left(\frac{\Gamma_{p_2}}{2}\right) \\ &\qquad \cdot \cos\left(\omega\tau - (k(2m-1)+m-1)\varphi\right), \\ N_1 &= \mathrm{d}D_1/\mathrm{d}\tau. \end{aligned} \tag{46}$$

It gives finally in a closed form that uses the notations introduced by equations (23), (24):

$$\begin{aligned} U_1(z,\tau) &= \frac{-1}{\mu\Gamma}\frac{f_1}{f_0\cos g_0}\sin(\omega\tau + g_1) \\ &\qquad \cdot \left(\varepsilon + \left(\frac{f_1}{2f_0\cos g_0}\right)^2 \varepsilon^3\right) + O(\varepsilon^4), \end{aligned} \tag{47}$$

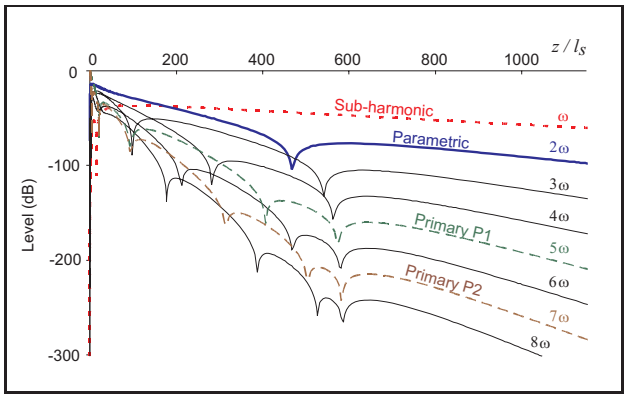


Figure 5. Evolution of the amplitude of the first 8 harmonics $U_n$ ($\mu = 3$, $\Gamma = 10$, $\varphi = 0$).

$$U_2(z,\tau) = \frac{1}{2\mu\Gamma}\left(\begin{array}{l}\left(\frac{f_1}{f_0\cos g_0}\right)^2 \sin(2\omega\tau + 2g_1)\varepsilon^2 \\ +\frac{1}{2}\left(\frac{f_1}{f_0\cos g_0}\right)^4 \sin(2\omega\tau + 2g_1)\varepsilon^4 \\ -4\frac{f_2}{f_0\cos g_0}\sin(2\omega\tau + g_2)\varepsilon^4\end{array}\right) + O(\varepsilon^4). \tag{48}$$

At very large $z$, one finds back the behavior described by equation (44), with the following coefficients:

$$U_1^{(\infty)} = \varepsilon\frac{-1}{\mu\Gamma}\frac{f_1}{f_0\cos g_0}\sin(\omega\tau + g_1) = \frac{2}{\Gamma\Omega}\frac{N_1}{D_0}, \tag{49}$$

$$U_2^{(\infty)} = \varepsilon^2\frac{1}{\mu\Gamma}\left(\frac{f_1}{f_0\cos g_0}\right)^2 \sin(2\omega\tau + 2g_1) = -\frac{2}{\Gamma\Omega}\frac{N_1 D_1}{D_0^2}. \tag{50}$$

Equation (49) translates the classical decreasing law that the sub-harmonic $\omega$ undergoes while propagating in an absorbing medium. On the other hand, equation (50) results from the nonlinear interaction of this sub-harmonic with itself, which feeds the wave at frequency $2\omega = \omega_-$. Therefore, the latter does not obey the thermo-viscous attenuation law.

Looking further at the evolution of the parametric wave, it can be checked that the second term in equation (48) is always negligible compared to the first one. The third term translates the contribution caused by the interaction of the two primary waves. The relative influence of the first and third terms is not obvious to delineate explicitly by analytical calculation. However, numerical simulations give a clear view of what happens. Figure 5 shows an example computed with $\mu = 3$ and $\Gamma = 10$ ($\varphi = 0$). It displays the evolution of the first harmonics obtained after the spectral analysis of $U(z,\tau)$. Note that the dynamic scale (300 dB) is not realistic with respect to experimental acoustic levels. This very large scale is used to observe clearly the asymptotic behavior of the various harmonics and to sort the different analytical contributions.

Two different zones can be observed for $U_2$. The farthest zone ($z > 600 l_s$) corresponds actually to the domain where the final ordering described by equations (44), (49) and (50) is settled. But there is an intermediate domain ($z < 400 l_s$) where the falling of the wave follows the classical absorption law, i.e. $\exp(-\alpha_{\omega_-} z) = \varepsilon^4$. The third term in equation (48) dictates the behavior of the parametric wave in this zone:

$$U_2(z,\tau) = -\varepsilon^4\frac{1}{\mu\Gamma}\frac{2f_2}{f_0\cos g_0}\sin\left(2\omega\tau + g_2\right) = \frac{2}{\Gamma\Omega}\frac{N_2}{D_0}. \tag{51}$$

This expression is identical to the efficiency defined by equation (29) when the parametric ratio $\mu$ is a half-integer. When $\mu$ is large, the approximation given by equation (40) can be also found back by keeping the first term in the series $N_2$ and $D_0$. Equation (51) corresponds to the contribution of the interaction between the only primary waves, which themselves undergo the extra attenuation phenomenon. This interaction is the root of the parametric transmission principle. The level of the secondary wave is significant in the first part of this zone. The asymptotic slope is ultimately altered by the existence of the subharmonic. However the transition occurs at such a distance that the secondary wave is already extinguished, i.e. below $-90$ dB in the presented case ($\mu = 3$), and still a lower level with higher parametric ratios. The subharmonic component rises to a significant level at a much shorter range than the distance where the transition occurs. In Figure 5, the sub-harmonic wave $\omega$ overcomes the parametric wave ($\omega_- = 2\omega$) at range $z = 170 l_s \approx 17 l_a$, the level being there only $-37$ dB below the strong initial primary level. This level may indeed carry a physical meaning, whereas the remaining part of the curves is rather of academic interest.

The generation of the sub-harmonic at frequency $\omega$ can be explained by observing the evolution of signal $U(z,\tau)$ along the $z$-axis. As for section 3.2, the initial wave is interpreted as the amplitude-modulated signal whose carrier frequency is $\Omega$, described by equation (42). The complete period of recurrence is equal to $T = 2\pi/\omega$. The period contains $q - p = 2$ envelopes, where the phase of the wave $\Omega$ shifts by $2\pi(\mu + 1/2)\mathrm{mod}2\pi = \pi$ from one envelope to the next. Figure 6 is computed with $\mu = 3$ and $\Gamma = 10$ ($\varphi = 0$). The reasoning is analogous to Figure 3. The phasing of the wave $\Omega$ is more appropriate in the first envelope than in the second one to build the parametric wave $\omega_-$. This lack of symmetry creates locally a variation in the efficiency of the conversion (see for example the frame computed at $z/l_s = 100$). It ends up by forming the wave at half the secondary frequency $\omega = \omega_-/2$.

## 5. Generalization

The study of integral and half-integral parametric ratios lets grasp what happens when the ratio $\mu$ is arbitrary. The creation of sub-harmonics can be linked to periodic variations of the efficiency of the parametric conversion. The initial wave can always be interpreted as an amplitude-modulated wave, as seen in equation (42) which is recalled

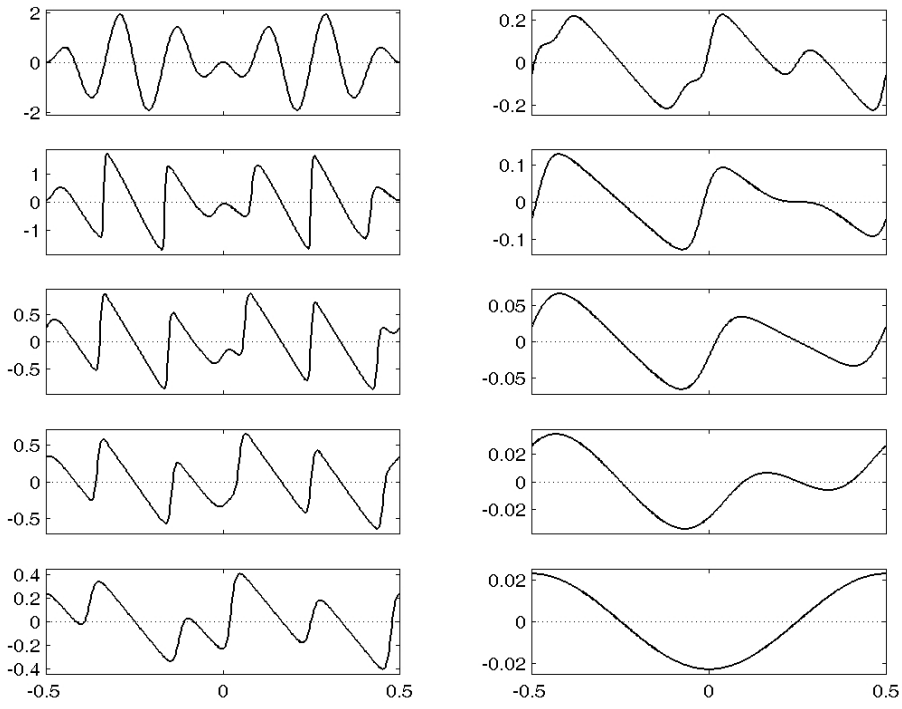


Figure 6. $\varepsilon^{-1}U(z,\tau)$ with $\mu = 3$ and $\Gamma = 10$ (normalized abscissa $\tau/T$). Left row, from top to bottom: $z/l_s$ = 0, 1, 3, 5, 10. Right row, from top to bottom: $z/l_s$ = 20, 50, 100, 200, $\infty$.

here explicitly:

$$U(z=0,\tau-\Delta\tau) = 2\cos\big(1/2(q-p)\omega\tau\big) \cdot \sin\big(1/2(q+p)\omega\tau - (\mu-1/2)\varphi\big). \tag{52}$$

The complete period of recurrence of this signal is $T = 2\pi/\omega$. The duration of each envelope is $T_e = 2\pi/((q-p)\omega)$. Hence within the complete period $T$, there are $(q-p)$ envelopes in which the carrier frequency $\Omega$ undergoes $(q-p)$ successive phase shifts. The phases influence locally the efficiency of the parametric conversion. The amplitude of the wave created at the difference frequency fluctuates, which ends up generating $(q-p-1)$ sub-harmonics. For example, let us consider the ratio $\mu = 2.51$ ($p = 201$, $q = 301$). This configuration is very close to the case $\mu = 2.5$ (section 3.2): the internal phasing of the initial carrier will scan $q - p = 100$ intermediate values. The local efficiency of the parametric conversion will fluctuate between $\eta_{\min}$ and $\eta_{\max}$ given by equations (32), (33) (see also Figure 2). The net result is thus a fading of the secondary level (about 10 dB when $\Gamma > 4$), whose period is 100 times the period of the parametric wave in this example.

The period corresponding to the carrier frequency $\Omega$ is $T_c = 4\pi/((q+p)\omega)$. So, the number of oscillations at the mean primary frequency $\Omega$ that a modulating envelope contains is equal to $T_e/T_c = \mu$. The influence of the phase is as much important as this number is small because the shapes of the signals within each envelope are very different. On the other hand, when the parametric ratio $\mu$ is large, there are many oscillations within each envelope: subparts of the signals are very similar, so that the variations of efficiency are weak, postponing to the very far range the effect of the sub-harmonics that are eventually created. Within the domain where the level of the secondary wave remains significant, and when $\mu \gg 1$, the parametric efficiency can be estimated by the approximation equation (40). However, it must be underlined that this approximation represents the theoretical asymptotic behavior only if the parametric ratio is a half-integer.

## 6. Conclusion

The presented study is based on analytical developments of the Burgers equation. It points out the influence of the phase of the primary waves on the efficiency of the parametric conversion, and the mechanism of sub-harmonic generation. The most important conclusion is that the parametric efficiency can fluctuate when the primary-to-secondary frequency ratio is small and is not an exact half integral number.

Numerical results are displayed to exemplify qualitative behaviors in the frame of a 1-D model. As presented in section 3.2, the effect of the initial phase can be significant at a range that is commensurate to the shock formation distance. Whenever this distance is commensurate to the Fraunhofer distance, the 1-D model gives a quantitative assessment of what happens in the nearfield of a parametric antenna, i.e. at a distance such that the primary field can be modeled as collimated plane waves.

Practical situations should be described with 3-D models, e.g. with the KZK equation that takes into account diffraction. However, the time-frequency representation used in the numerical implementation of such models must be sufficiently accurate so as not to overlook the phase ef-

fect. Nevertheless subharmonic generation should appear in 3-D through the same mechanism as in the 1D model, so that the presented simple 1D model is interesting to detect which practical situations can be prone to experimental evidence.

Practically, parametric antennae are designed to obtain a compromise between efficiency and directivity. Optimal solutions lead to rather small parametric ratios $\mu$ (let say less than 6). Because the initial phasing has a possible influence in this case, a special attention must be taken in the shape of the source signals that are actually used.

## References

[1] P. J. Westervelt: Parametric acoustic array. J. Acoust. Soc. Am. **35** (1963) 535–537.

[2] M. F. Hamilton, D. T. Blackstock (eds.): Nonlinear acoustics. Academic Press, 1998.

[3] J. M. Burgers: A mathematical model illustrating the theory of turbulence. Adv. Appl. Mech. **1** (1948) 171–199.

[4] D. T. Blackstock: Thermoviscous attenuation of plane, periodic, finite-amplitude sound waves. J. Acoust. Soc. Am. **36** (1964) 534–542.

[5] O. V. Rudenko, S. I. Soluyan: Theoretical foundations of nonlinear acoustics. Plenum, New-York, 1977. Chap. 6 section 2.

[6] B. K. Novikov, O. V. Rudenko, V. I. Timoshenko: Nonlinear underwater acoustics. American Institute of Physics (Acoustical Society of America translation book), New York, 1987.

[7] C. M. Hedberg: Multifrequency plane, nonlinear, and dissipative waves at arbitrary distances. J. Acoust. Soc. Am. **106** (1999) 3150–3155.

[8] C. M. Hedberg: A multi-frequency solution for the Burgers equation. – In: Nonlinear acoustics at the turn of the millennium. American Institute of Physics, New-York, 2000, 15th ISNA, 125–128.

[9] B. K. Novikov: Exact solutions of the Burgers equation. Sov. Phys. Acoust. **24** (1978) 326–328.

[10] E. Hopf: The partial differential equation $u_t + uu_x = \mu u_{xx}$. Commun. Pure Appl. Math. **3** (1950) 201–230.

[11] J. D. Cole: On a quasilinear parabolic equation occurring in aerodynamics. Quat. Appl. Math. **3** (1951) 225–236.

[12] C. M. Hedberg: Influence of phase between original frequencies on the nonlinear generation of new harmonics. Examples of application from nonlinear acoustics. J. Acoust. Soc. Am. **99** (1996) 3329–3333.

[13] R. D. Fay: Plane sound waves of finite-amplitude. J. Acoust. Soc. Am. **3** (1931) 222–241.